1 **Supplementary Information for**

2

3 **An ABCC-type transporter endowing glyphosate resistance in plants**

4 Lang Pan, Qin Yu[*], Junzhi Wang, Heping Han, Lingfeng Mao, Alex Nyporko, Anna

5 Maguza, LongJiang Fan, Lianyang Bai[*], Stephen Powles[*]

6

7 [*]co-correspondence authors:

8 Qin Yu, qin.yu@uwa.edu.au; Lianyang Bai, lybai@hunaas.cn; Stephen Powles,

9 stephen.powles@uwa.edu.au.

10

11

12 **This PDF file includes:**

17

18

SI Materials and Methods

Plant material

Glyphosate resistance in an *Echinochloa colona* population studied here has been characterized (1, 2). Glyphosate resistant (GR) and susceptible (S) *E. colona* lines/populations used in this current study were described in our previous work (3).

RNA-seq data analysis and selection of candidate transporter contigs

RNA-seq was conducted to select for relevant membrane transporter genes using R and S lines isolated from within a single GR population. The RNA-seq experiment, data analysis, qPCR validation of the candidate genes in RNA-seq samples, and samples from multiple GR and S populations/lines and under different temperatures, were the same as described (3). Candidate transporter gene contigs were selected on the basis of statistical significance ($p<0.05$), magnitude of expression difference (fold change >1.5), and annotations with putative assignment to membrane transporters. Shoot material of GR and S plants was used for RT–qPCR validation and primers (*SI Appendix*, Table S1) were assessed for specificity to amplify a single PCR product with efficiencies between 84–115%. Leaf, stem and root tissues of 10 R and S plants (at the three- to four-leaf stage) were also separately harvested for RT-qPCR investigation of *EcABCC8* expression patterns. Each experiment included three biological replicates and was repeated at least twice.

Rice genetic transformation with the two ABC transporter genes *EcABCC8* and *EcABCC10*

Based on *Echinochloa crus-galli* genome sequences (4), two primer pairs EcABCC8-F (5'-CATGTCCTGATACAATGGTAGG-3')/ EcABCC8-R (5'-GCGGCAATGGCAGATAAG-3') and ECABCC10-F (5'-CGTGCGTCGGAACAAGAA-3')/ ECABCC10-R (5'-CCCGACAAACGAGCCAAA-3') were designed from the UTR (Untranslated Region) to clone the full CDS of the two *E. colona* ABC transporter contig genes (EC_v4.g098055 and EC_v4.g102032). The primer pair (F: 5'-GGCGGGGATAAAGAACAC-3', R: 5'-GCCGATTAGGATGGAGTG-3') was designed to amplify the full region upstream of the *EcABCC8* ATG start codon (promoter

sequence) from genomic DNA of the GR and S *E. colona* plants. The resulting 1990 bp amplicon was validated by sequencing.

The two *E. colona* ABC transporter genes (named as *EcABCC8* and *EcABCC10*) were inserted into the transformation vector pOX under the 35S promoter to generate the *EcABCC8* expressing (*EcABCC8*-OE) and *EcABCC10* expressing (*EcABCC10*-OE) vectors (*SI Appendix*, Fig. S13). These recombinant vectors were used to transform the rice cultivar Nipponbare by *Agrobacterium tumefaciens*-mediated transformation. Generation of T1 *EcABCC8-OE* and *EcABCC10-OE*, and T2 *EcABCC8-OE* lines were described in our previous work (3). The T1 and T2 *GFP*-control (*GFP*) rice lines (3) were used as controls. Heterologous expression of *EcABCC8* and *EcABCC10* in transgenic rice was confirmed by successful PCR amplification of the vector HPT gene (3).

For evaluation of glyphosate sensitivity, the transgenic rice lines were grown in pots containing potting mix in a growth chamber with day/night temperature of 30/25°C and a 14-h photoperiod at a light intensity of 180 μmol m^{-2} s^{-2} (3). At the three- to four-leaf stage, they were foliar treated with glyphosate at 540 g ha^{-1} (the recommended field rate) using a 3WP-2000 hand-held system (Zhongnongjidian, China). Glasshouse glyphosate dose response experiments were conducted to quantify the resistance level using the four-leaf stage seedlings of one homozygous T_2 line of *EcABCC8*-OE. There were three replicate pots for each treatment and 8-10 plants per pot. Above-ground plant material was harvested and fresh weight determined three weeks after treatment. The herbicide rate causing 50% growth reduction (GR_{50}) was estimated by fitting data to the four-parameter log-logistic model using SigmaPlot 13.0 (Systat Software, Inc., San Jose, USA) as described (5). Significant difference in GR_{50} values between treatments was tested by Prism.

Homologous overexpression of *EcABCC8* orthologs in other crop plants

The *Oryza sativa* gene (LOC_Os06g36650) is orthologous *to the EcABCC8* gene. The 3588-bp CDS was amplified (named as *OsABCC8*) and ligated into the pOX vector with *Kpn*I and *Mlu*I restriction sites (*SI Appendix*, Fig. S13) for *A. tumefaciens* transformation using the procedures as described (3, 6). The *OsABCC8* transcript level was found to be 26-fold higher in *OsABCC8*-OE than in GFP rice by RT-qPCR

1 using gene specific primers. T$_1$ rice seedlings (*OsABCC8*-OE) were grown in pots in a

2 greenhouse at 28°C with a 14-h photoperiod, and the pots were placed in large

3 plastic trays with regular watering. Plants at the five- to six-leaf stage were

4 glyphosate treated.

5 A 4482-bp CDS of the orthologous gene in *Zea mays* (Zm00001d046226) was

6 amplified (named as *ZmABCC8*), and cloned into the binary vector NEWMOL to

7 generate the NEWMOL-*ZmABCC8* construct with *Sac*I and *BamH*I restriction sites (*SI*

8 *Appendix*, Fig. S13) for *A. tumefaciens* transformation (7). The *ZmABCC8* gene was

9 27-fold higher expressed in *ZmABCC8*-OE than in the wildtype (WT) maize seedlings.

10 T$_1$ maize seedlings were grown under the same conditions as rice, and the four- to

11 five- leaf stage plants were used for glyphosate treatment.

12 A 4394-bp CDS of the orthologous gene in *Glycine max* (Glyma.07G011600.1) was

13 amplified (named as *GmABCC8*), and cloned into the pCAMBIA3301 vector

14 containing a CaMV 35S promoter and a *bar* gene (*SI Appendix*, Fig. S13) for *A.*

15 *tumefaciens*-mediated hairy root transformation (8). The *GmABCC8* transcript level

16 was 22-fold higher in *GmABCC8*-OE than in WT soybean seedlings. T$_1$ soybean

17 seedlings were grown at 25°C with a 16-h photoperiod for two weeks before being

18 transferred to the glasshouse under the same conditions as rice, and the five- to

19 six-leaf stage plants were glyphosate treated.

20 The field rate of glyphosate (540 g ha^{-1}) was first used to test the sensitivity of these

21 crop plants overexpressing *EcABCC8* orthologs, and then growth response to a range

22 of glyphosate rates was measured to quantify the resistance levels as described

23 above for EcABCC8 transgenic rice.

24

25 **Rice *OsABCC8* gene knockout by CRISPR/Cas9 gene editing**

26 The non-functional *OsABCC8* knock out (*OsABCC8*-KO) rice lines were generated

27 using CRISPR/Cas9. A 19-bp targeting sequence was selected and the targeting

28 specificity was confirmed using a Blast search against the rice genome

29 (http://blast.ncbi.nlm.nih.gov/Blast.cgi) (9) , and then integrated into the pBGK032

30 vector. The CRISPR/Cas9 plasmids were introduced into *A. tumefaciens* strain

31 EHA105. Rice transformation was performed as described previously (10). Genomic

32 DNA was extracted from these transformants and primer pairs flanking the designed

target site were used for PCR amplification. The PCR products were sequenced directly and identified using the Degenerate Sequence Decoding method (11). The *OsABCC8* gene was sequenced in all T_1 transgenic lines, and homozygous mutants identified to generate 12 T_2 homozygous *OsABCC8* KO lines (six for *osabcc8-1* and six for *osabcc8-2* variant lines) and sequenced again for confirmation.

For glyphosate response, T_2 seedlings of the two non-functional KO variant lines (*osabcc8-1* and *osabcc8-2*) at the three- to four-leaf stage, were foliar treated with glyphosate at 26, and 105 g ha^{-1}, respectively. Then growth response (GR$_{50}$) to glyphosate (0, 16, 31, 63, 135, 270, and 540 g ha^{-1}), was measured to estimate the magnitude of changes in glyphosate sensitivity. There were five seedlings per pot and three replicate pots per treatment per KO line.

Global DNA methylation analysis for *E. colona*

Genomic DNA was extracted from the GR and S shoot material using the Qiagen DNeasy Plant Minikit. MethylC-seq libraries were prepared as described (12, 13) and three biological replicates were used per sample. Clean BS-seq reads were mapped to the reference genome of *E. crus-galli* (4), with the Bisulfite Sequence Mapping Program (BSMAP) aligner (14). Calculation of methylation status of each cytosine in *E. crus-galli* genome and binomial test using the false discovery rate (FDR) for each cytosine base in the *E. crus-galli* genome was performed as described (15). Only cytosines covered with at least four reads in a library were considered to identify DMRs (differentially methylated regions). Cytosines (Cs) or thymines (Ts) were counted separately in each sliding window for three sequence contexts (CG, CHG, or CHH). The methylation level for a sliding window and DMRs was determined as described (16). DNA methylation levels of different libraries were compared pairwise using Fisher's exact test, and *p*-values were adjusted for multiple comparisons using the Benjamini–Hochberg method.

Subcellular localization of ABCC8

The full CDS of *EcABCC8* (except for the stop codon) was cloned into the pMD19-T simple vector for sequence confirmation and then cloned into the vector pBWA(V)HS580 to produce a fusion gene with GFP under control of the CaMV35S

promoter, using the Clonetech in-fusion PCR cloning system (TaKaRa). The plasmid pBWA(V)HS580-*35S:EcABCC8-GFP* was used for rice protoplast transformation with pBWA(V)HS580-*35S:GFP* as a background control, pBWA(V)HS580-*35S:SCAMP1-mRFP* as a PM protein marker (17) and pBWA(V)HS580-*35S:AtTPK3-mRFP* as a tonoplast marker. Rice (Nipponbare) and Arabidopsis seeds were germinated and cultured for 8 d on 1/2 MS culture medium at 28 °C under continuous light. Shoot material (2 mm sections) for rice (18) and arabidopsis (19) were used for protoplast isolation. Ten microgram plasmids of *35S:EcABCC8-GFP* and *35S:SCAMP1-mRFP*, *35S:EcABCC8-GFP* and *35S:AtTPK3-mRFP* or *35S:GFP* alone were mixed with 220 µl 40% (0.4 g ml^{-1}) PEG-4000 and used for transformation of protoplasts (200 µl) with 16 h incubation in the dark. For each treatment, >20 individual cells were imaged by MCLSM. The PM location of the maize ortholog GmABCC8 was determined following the same protocol as for EcABCC8.

Glyphosate efflux and content in leaf discs of transgenic rice seedlings

Glyphosate efflux and content at the cellular level was investigated using leaf discs. Two-leaf stage transgenic rice T_2 seedlings, *EcABCC8*-OE versus *GFP* and *OsABCC8* KO (*osabcc8-1*) versus WT, were used. Two fully expanded young leaves were collected from each plant (n = 5 plants) and surface sterilized with 70% ethanol. Six leaf discs toward the base of each leaf (avoiding taking the midrib) were sampled from each leaf using a 1 mm cork borer. Each set of the 60 fresh leaf discs were weighed and vacuum infiltrated using a 20 mL syringe with 5 mM ammonium phosphate buffer (pH 5.5) containing 0.1% (v/v) Tween 80 and 10 mM sucrose. The infiltrated leaf discs were kept in the buffer medium at RT in low light conditions until used.

Glyphosate incubation and efflux were carried out using described procedures (20, 21). Briefly, infiltrated leaf discs of each replicate (60 leaf discs per replicate and three replicates per time point) were transferred into plastic wells containing 5 mL 60 µM glyphosate and incubated for 24 h at 25°C with gentle stirring. The leaf discs were then rapidly rinsed with fresh buffer medium and an aliquot of the solution medium was removed from the wells at various time intervals (2.5, 5, 10, 15, 30, 60 and 90 min), and the glyphosate concentration measured in the aliquots using

HPLC-Q-TOF-MS (3). After completion of the efflux experiment, glyphosate was extracted from leaf discs in 10% (v/v) cold methanol and measured by UPLC-MS/MS (3).

The glyphosate efflux to the external medium was estimated using a modified hyperbola model y=at/1+bt (SigmaPlot 13.0, Systat Software, San Jose, CA, USA). Where y= amount of glyphosate in the medium, a= asymptotic value, b= increase rate of the amount of glyphosate for a given increase in efflux time, and t= efflux time. Significant difference in efflux rates (b) between treatments is tested by the Prism. The experiment was repeated with similar results.

Glyphosate quantification in leaf protoplasts of transgenic rice plants

Shoot material of three- to four-leaf stage seedlings (two T_2 *EcABCC8*-OE rice lines versus the *GFP*, and two *OsABCC8* KO lines versus the WT) were used for experiments. For *in vivo* glyphosate treatment, seedlings were first foliar sprayed with glyphosate at 68 g ha^{-1} (one eighth of the recommended field rate) and then protoplasts isolated 2 and 6 h after treatment following a published protocol (18) and kept at -80 °C. Unabsorbed glyphosate on the shoot material was removed by washing in deionized water for 3 min. Protoplast number was estimated under the microscope with a hemocymeter and intactness (81-86%) evaluated by fluorescence staining using fluorescein diacetate (FDA) (22). Samples were refluxed in 1N H_2SO_4 at 90 °C for 2 h, followed by centrifugation at 10,000*g* (23), and the supernatant was used for glyphosate quantification using HPLC-Q-TOF-MS (3).

In vitro glyphosate treatment followed an established protocol (24) with modifications. Glyphosate was added to 5 ml protoplast preparation (in MES buffer, pH 5.6) at a final concentration of 60 μM. The protoplast suspension was gently and constantly stirred on a reciprocal shaker during the treatment at 28°C. One and 2h after glyphosate treatment, 0.4 ml of the protoplast suspension was sampled from the incubation medium and overlaid on a 0.5 ml cushion of silicon oil. Treated protoplasts (83-86% intactness) were separated from the incubation medium and silicon oil by centrifugation for 2 min at 6,500*g,* and the pellet was solubilized overnight at 55°C in a mixture of 0.1% Triton-X-100, HClO$_4$ and 30% H_2O_2. After

1 centrifugation, the supernatant was used for quantification.

2 For time-dependent glyphosate accumulation in protoplasts, one T_2 *EcABCC8*-OE rice

3 line versus the *GFP* was used, and 0.4 ml of the protoplast suspension were sampled

4 5, 10, 20, 40, 60, 80, 100 and 120 min after glyphosate treatment. The primary

5 glyphosate metabolite AMPA (60 μM) was used as a control following the same

6 treatment procedure as glyphosate. HPLC-Q-TOF-MS (3) was used for quantification

7 of AMPA.

8 About 2-4 g shoot material was used for each protoplast preparation with three

9 biological replicate preparations and two technical replicates per treatment.

10 Significant difference in glyphosate levels between treatments was tested by Prism.

11 The time-dependency experiments were repeated with similar results.

12

13 **Structural reconstruction of *EcABCC8* variant**

14 Spatial structure of full-length EcABCC8 in the inward-facing and outward-facing

15 (open and close) conformations was reconstructed with combination of homology

16 modelling approaches (using desktop Modeler software and SwissModel web service)

17 (25, 26) and *ab initio* approaches (using Robetta web-service for reconstruction of

18 TMD0 spatial structure and the loop between the TMD0 and TMD1 domains). The

19 search and scoring of structural templates were performed via internal tools of

20 (Modeller/SwissModel/Robetta) as well as web-service HHPred based on the

21 pairwise comparison of hidden Markov models (HMMs) profiles (27, 28). The spatial

22 structures of bovine MRP1 (29, 30) in an open (PDB access code 5uja) and closed

23 (PDB access code 6bhu) status were used as base templates for reconstruction of the

24 inward-facing and outward-facing conformation of EcABCC8, respectively. These

25 entries revealed the highest scores among all possible structural templates. The

26 extremely similar distribution of secondary structure elements between EcABCC8

27 and MRP1 sequences (28) and similar domain architecture (31) are additional

28 indicators of 3D structural similarity between these homological proteins.

29 Blind docking of the glyphosate molecule into the EcABCC8 surface was performed

30 with the S4MPLE software (32) that uses hybrid genetic algorithms combining

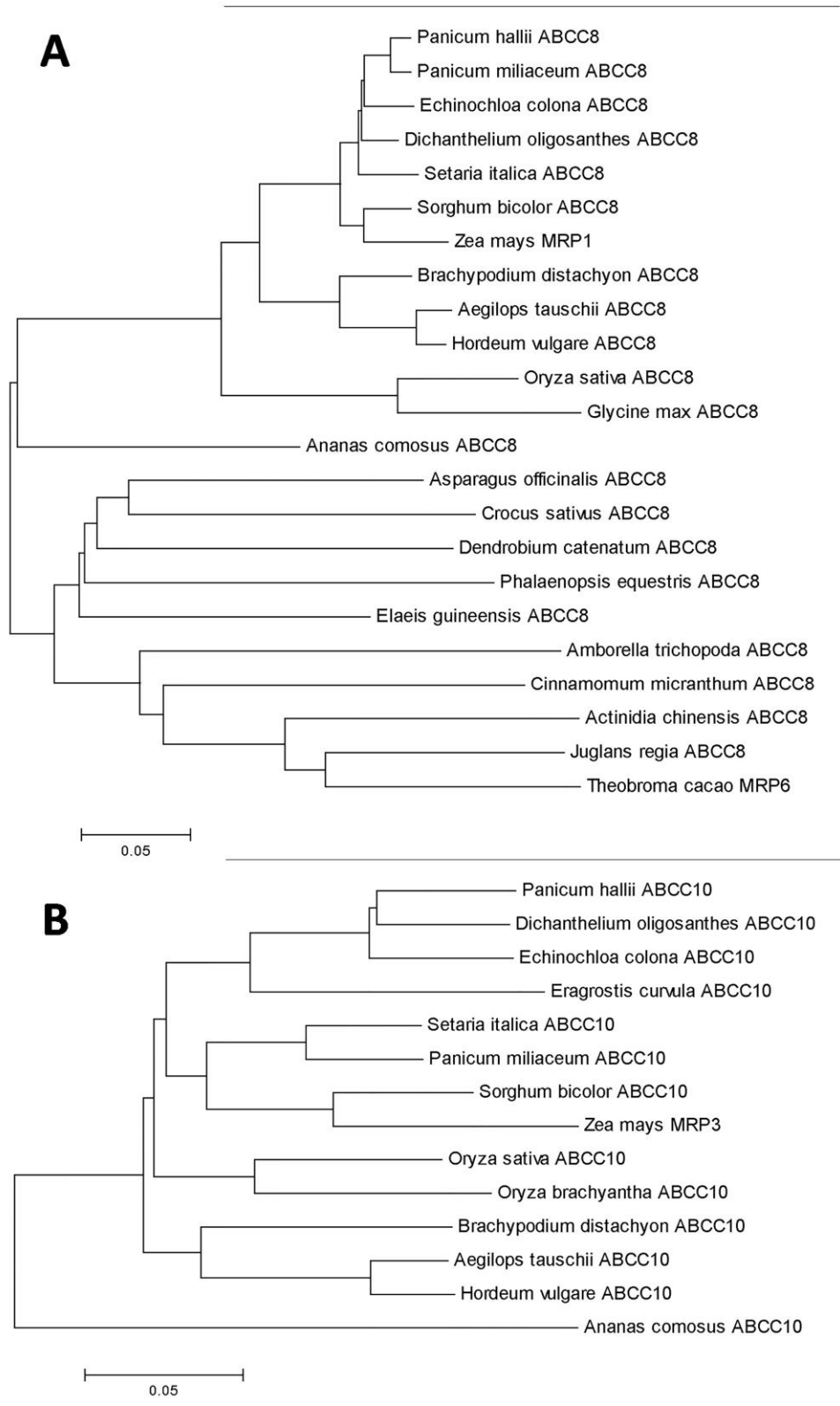31 molecular modelling-specific optimization with classical evolutionary sampling

strategies and especially specified for accurate prediction and evaluation of binding patterns. The docking procedure used the following parameters: size of population *npop*=30, number of generation *ngen*=300, minimal differences for interaction fingerprint of two non-redundant conformers (related to fingerprint size) *minfpdiff*=0.01. All on-surface exposed residues except lipid-contact ones were used as hotspots for docking. To confirm the localization of glyphosate binding site(s) the alternative docking was also performed with the FlexX software (BioSolveIt, www.biosolveit.de) that uses knowledge-based scoring functions instead of force field-based scoring in S4MPLE. Two hundred iterations per search with 200 maximum solutions per iteration were used, and the maximal 2.9 A protein-ligand clash and 0.5 A intra-ligand clashes are considered to be acceptable. Both software placed the best scoring solutions at the same sites on the protein surface, and the RMSD between them does not exceed 0.6 A. The glyphosate topology for application in molecular dynamics (MD) simulations was performed via the web-based tool Swiss Param (33).

The integration of EcABCC8-glyphosate complexes into bilipid membrane, periodic box generation and solvation of the studied molecular systems were performed with CHARMM-GUI web service (34). The orientation of EcABCC8 in PM, borders and thickness of the membrane were calculated with PPM web server (35). A lipid composition of PM was reconstructed using Membrane Builder tool of CHARMM-GUI. The energy minimisation of the studied systems was carried out using LBFG algorithm (36), position restrained MDs for canonical NVT (N for particle number, V for volume, T for temperature) and isothermal-isobaric NPT (P for pressure). Ensembles were calculated within 100 ps intervals (to achieve the equilibrate state), and the unrestrained (productive) MD within 150 ns time intervals at 300K. All MD calculations were performed with the Gromacs software (37). Computational details correspond to a MD procedure described in our previous work (38). Moving of glyphosate molecule to and from the binding site(s) was calculated using a steered dynamics approach (39) with the rate of the reference position change of 0.01 A per ps and force constant of 1000 kJ $mol^{-1}nm^{-2}$.
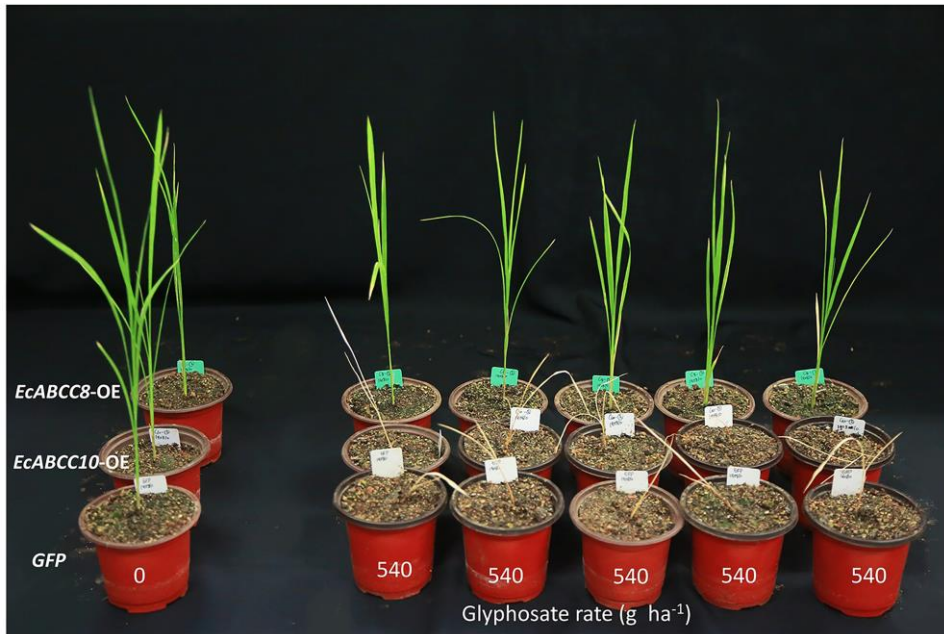
**Figure S1.** Phylogenetic analysis of *EcABCC8* (A) and *EcABCC10* (B). MEGA6 was used for the tree construction using the neighbor joining method and clustal W program, with boot strap method taking 500 replicates. The branch number (0.05) refers to the bootstrap confidence.

Figure S2. Resistance and susceptibility to glyphosate of transgenic rice. Growth response to glyphosate of T$_1$ rice seedlings expressing *EcABCC8* (*EcABCC8*-OE) or *EcABCC10* (*EcABCC10*-OE), relative to the *GFP* control, recorded three weeks after glyphosate treatment. Note expression of the *EcABCC10* gene does not confer glyphosate resistance in rice transgenic lines. Only glyphosate surviving T$_1$ seedlings from *EcABCC8*-OE lines were shown.
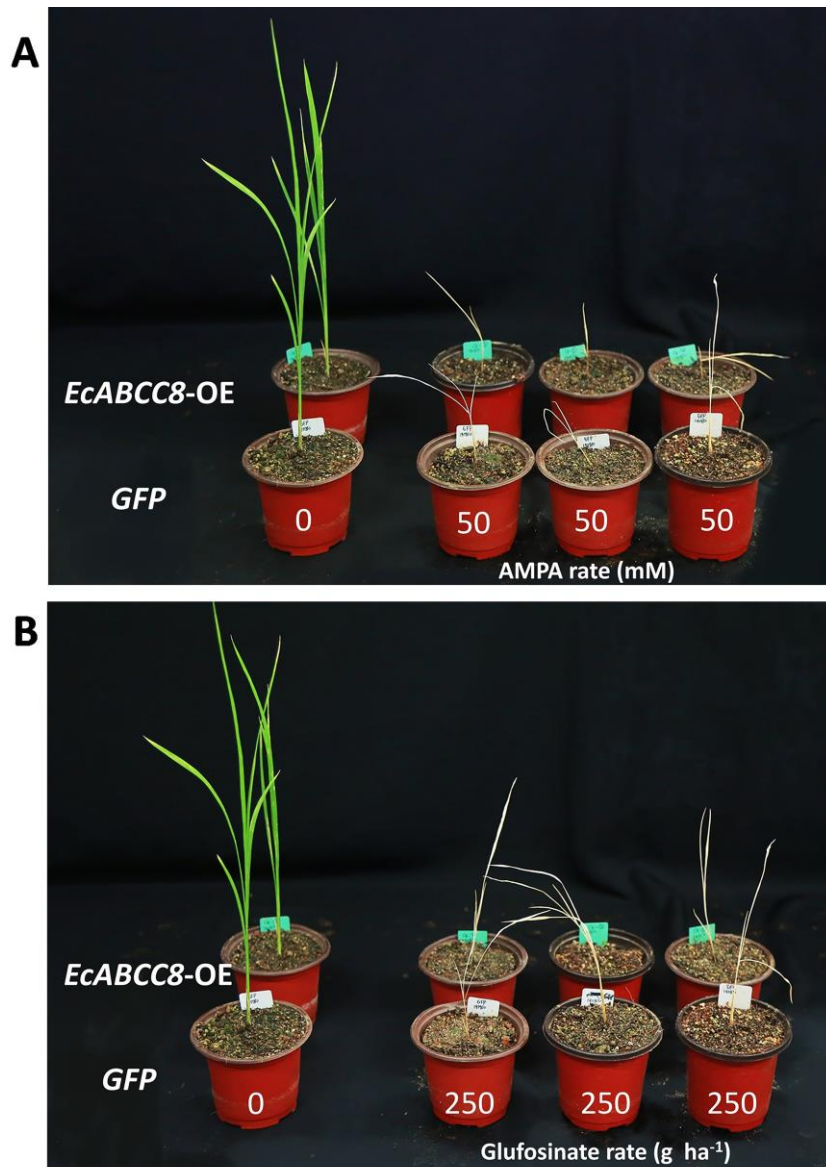
Figure S3. Response of transgenic rice to other compounds. Growth response to the glyphosate metabolite AMPA (A), and glufosinate (B) of T_1 rice seedlings expressing *EcABCC8* (*EcABCC8*-OE) versus *GFP* control, recorded three weeks after treatment.
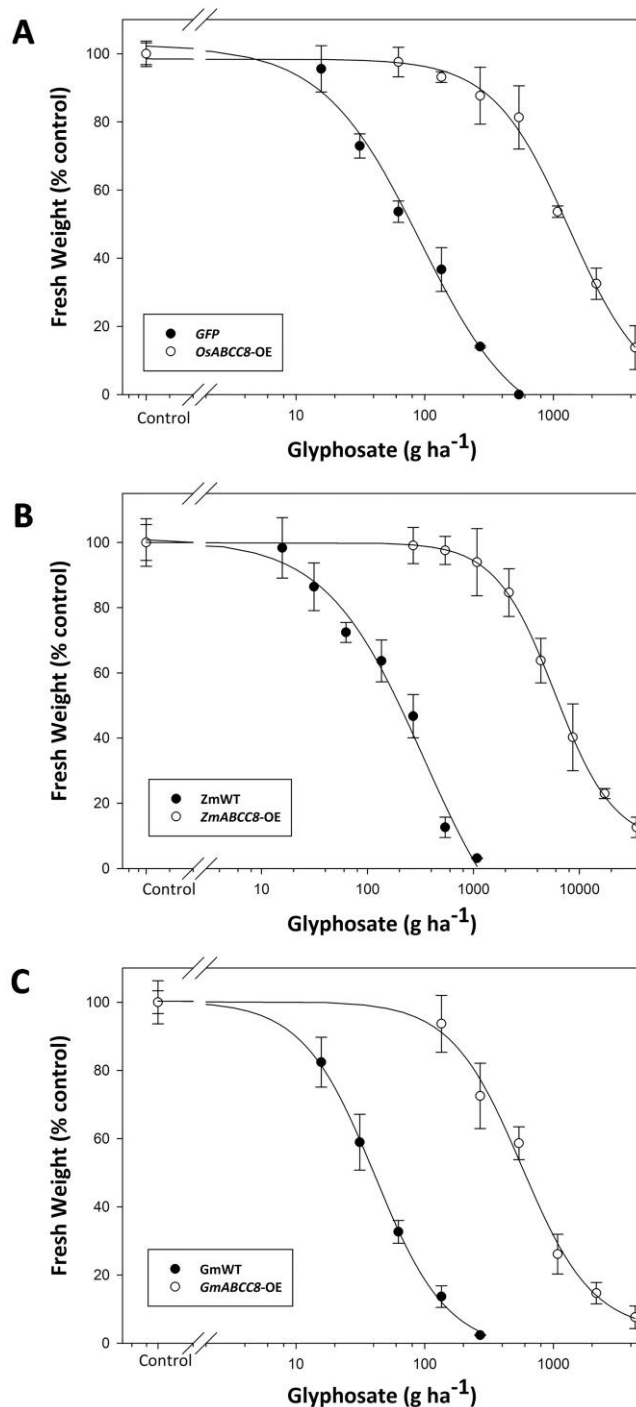
Figure S4. Glyphosate dose responses of transgenic crops overexpressing *EcABCC8* ortholog genes. (A) *OsABCC8* (*OsABCC8*-OE) in rice, (B) *ZmABCC8* (*ZmABCC8*-OE) in maize, and (C) *GmABCC8* (*GmABCC8*-OE) in soybean, relative to the *GFP* or untransformed WT controls. Plants at the four- to six-leaf stage were foliar sprayed with glyphosate, and results assessed three weeks after treatment. Data points are means ± SE (*n*=3).
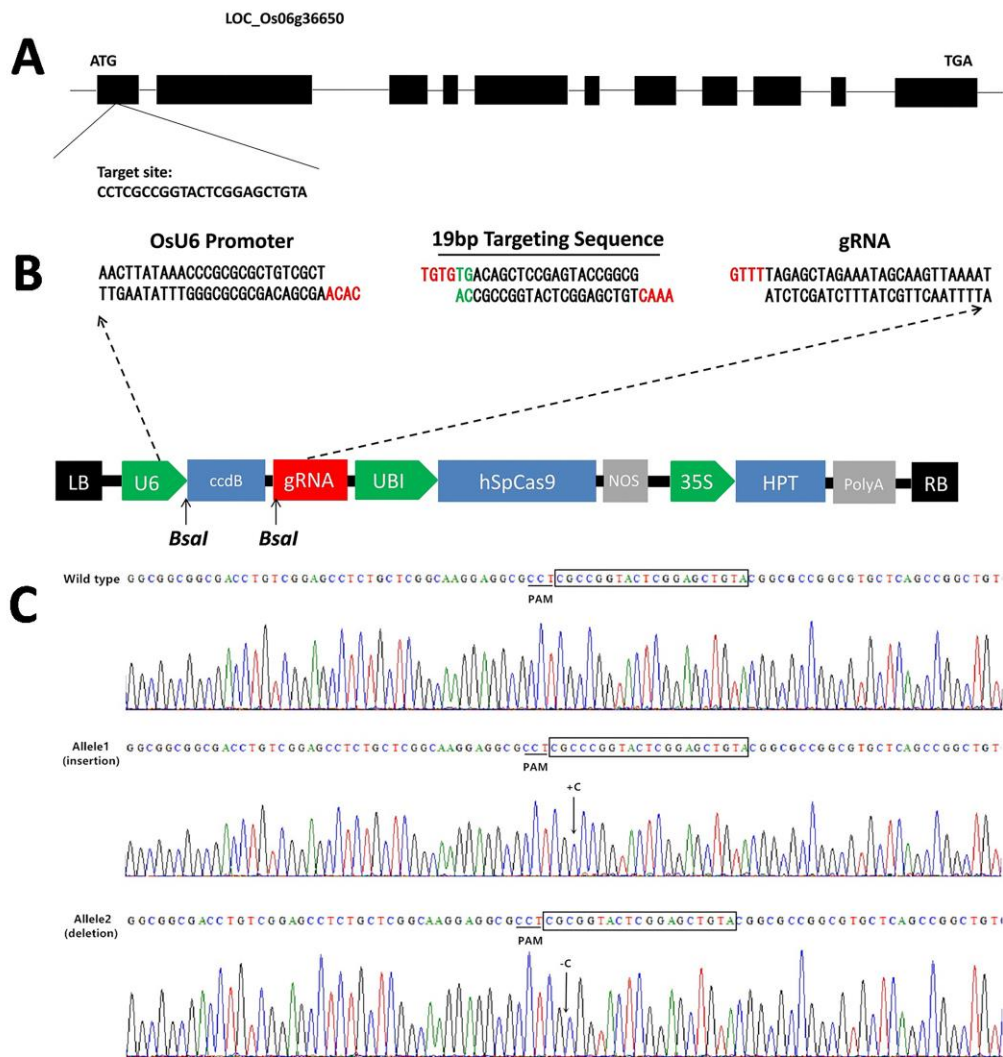
Figure S5. CRISPR/Cas9-induced *OsABCC8* (LOC_Os06g36650) gene editing in rice. (A) Schematic of the LOC_Os06g36650 gene structure and target site. Exons and introns are indicated with black rectangles and black lines, respectively. (B) Structure of the CRISPR/Cas9 binary vector pBGK032. The key sequences and restriction sites for cloning are given. The expression of Cas9 is driven by the maize ubiquitin promoter (UBI); the expression of the sgRNA scaffold is driven by the rice U6 small nuclear RNA promoter (OsU6), and the expression of hygromycin (HPT) is driven by CaMV35S promoters (35S). Abbreviations: NOS, gene terminator; LB and RB, left border and right border, respectively. (C) Nucleotide sequences at the target site in the nine T_0 rice mutants. The recovered mutant allele sequences are shown below the wild type sequence. Target site nucleotides are in black boxes and the protospacer adjacent motif (PAM) site is underlined. The inserted (Allele 1) or deleted (Allele 2) nucleotide is arrowed.

14
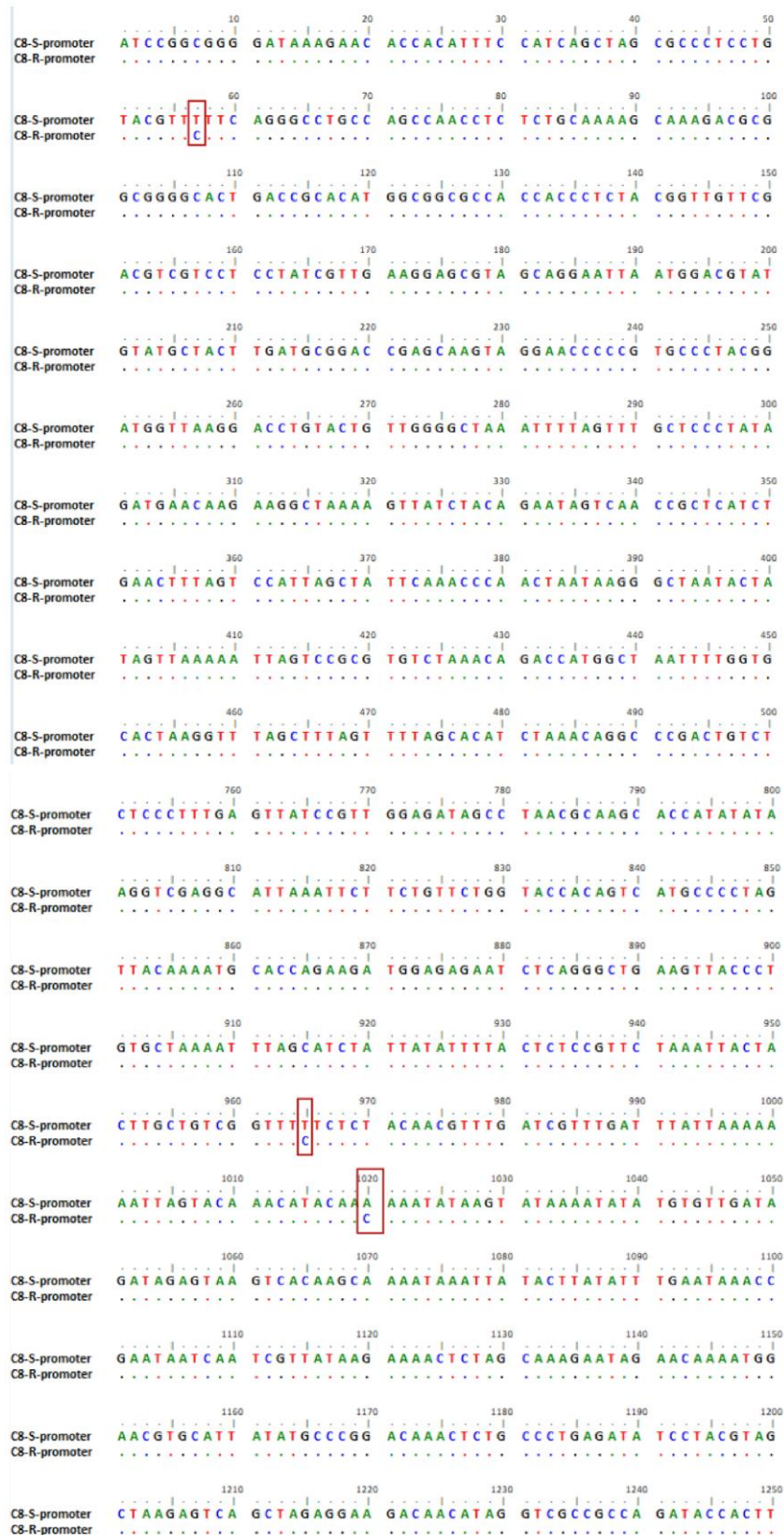
Figure S6. Comparison of the amplified *EcABCC8* promoter sequences from glyphosate resistant (GR) and susceptible (S) *E. colona* plants. Single nucleotide polymorphisms are boxed.
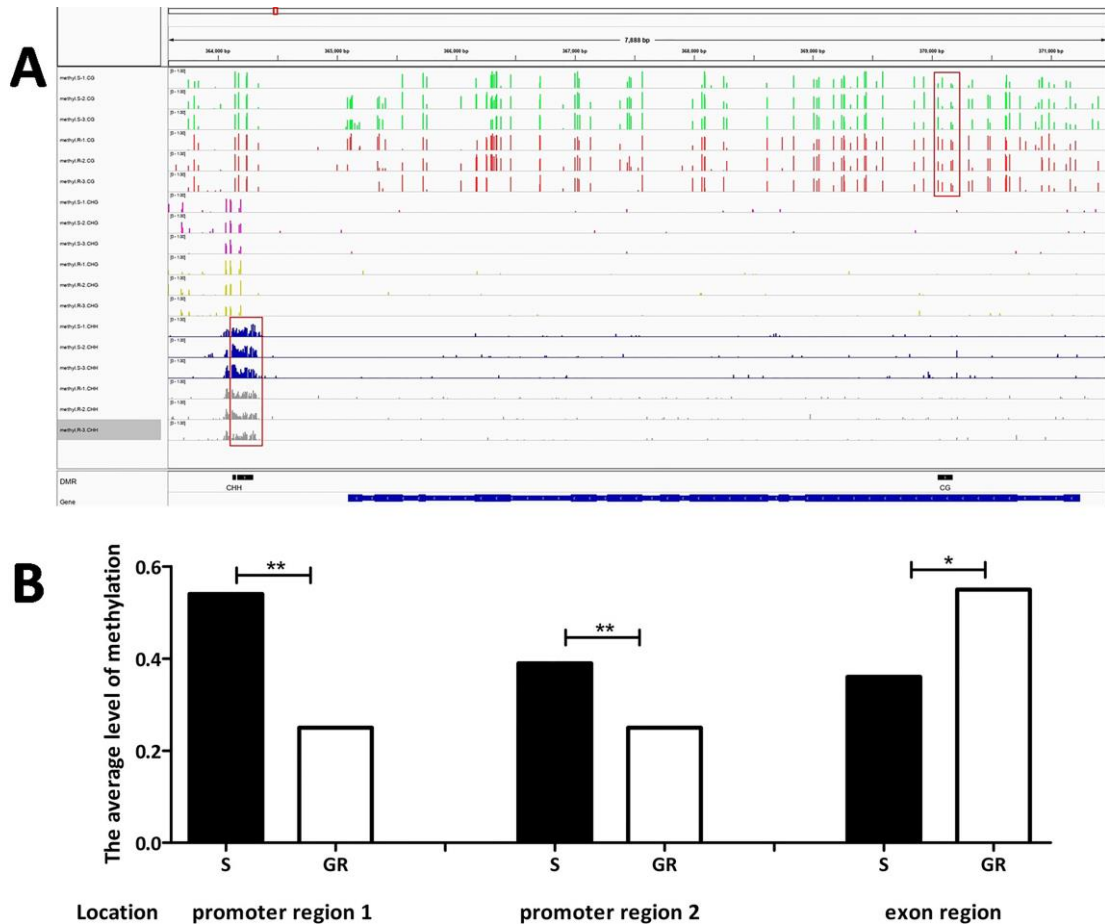
Figure S7. Global methylation analysis of the *EcABCC8* gene in S versus GR *E. colona* samples. (A) Differentially methylated regions (DMRs) are proximal to the upstream (promoter) and exon regions of the *EcABCC8* gene (EC_v4.g098055) (S versus GR). Significant difference in CHH and CG methylation ($p < 0.05$; Student's *t*-test) is shown in box. (B) Differentially DMRs of the *EcABCC8* gene between the S and GR plants in two promoter (CHH methylation) and one exon (CG methylation) regions. Significance of difference by the student t-test is indicated by *($p<0.05$) and **($p<0.01$).
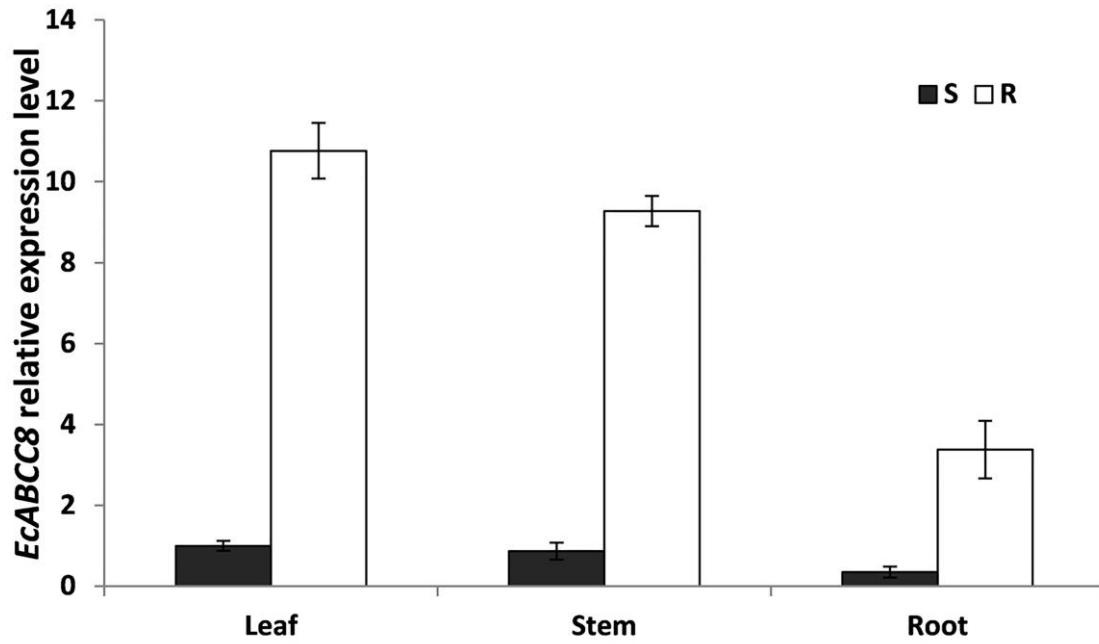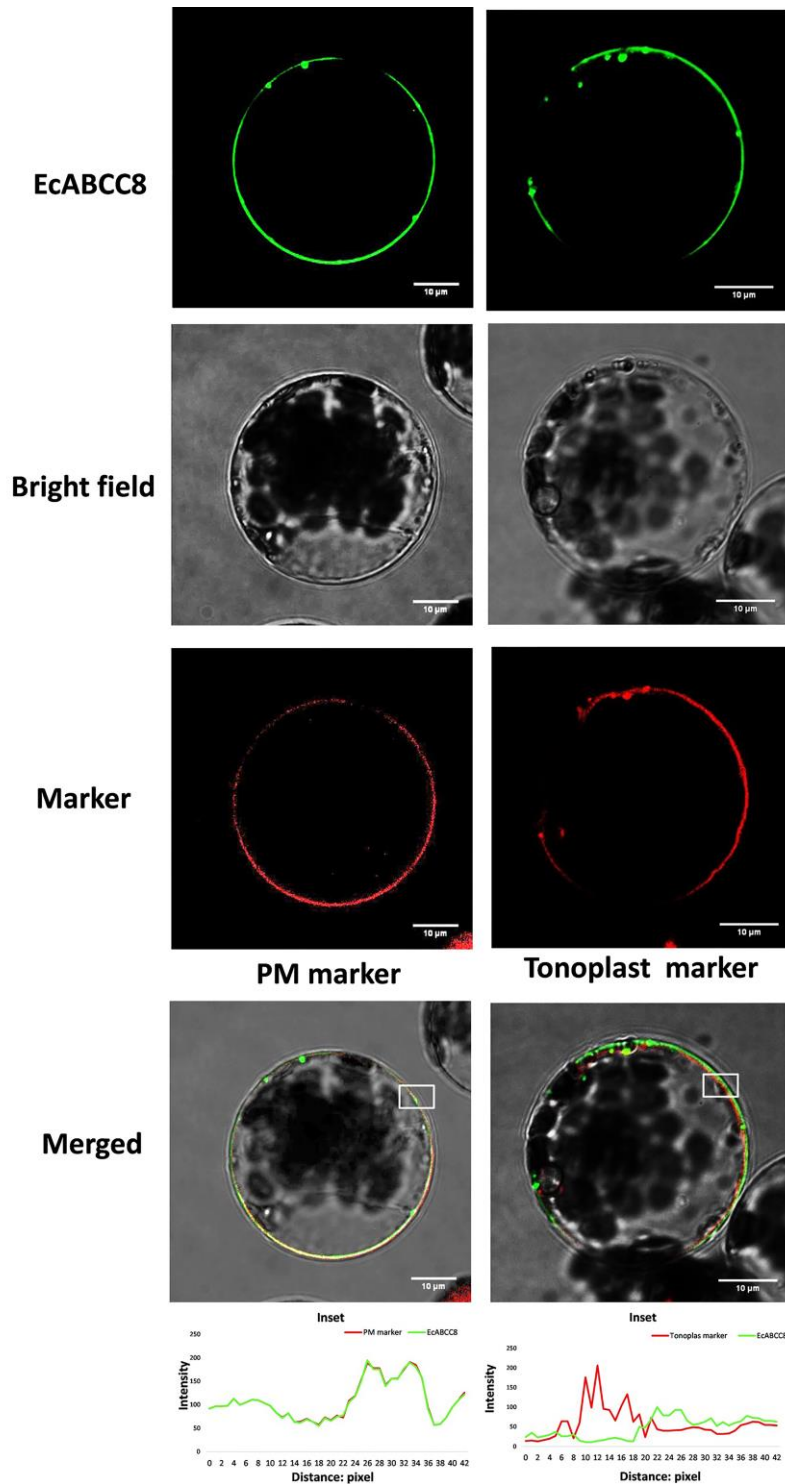
Figure S8. Tissue expression of EcABCC8. Relative expression levels of *EcABCC8* in the leaf, stem and root tissue of GR and S *E. colona* plants. Data points are means ± SE (n=3). Gene expression level in the leaf tissue of S plants was set as 1.

Figure S9. Subcellular location of EcABCC8 in Arabidopsis protoplasts. Co-localization of the EcABCC8 and the plasma membrane (PM) marker, and lack of co-localization of the EcABCC8 and the tonoplast marker. Linescan analysis showing overlapping of fluorescence distribution of EcABCC8 (green) and the PM maker (red) (left panel), and separation of EcABCC8 (green) and the tonoplast marker (red) (right panel) in areas of interest (boxed). Scale bars: 10 μm.
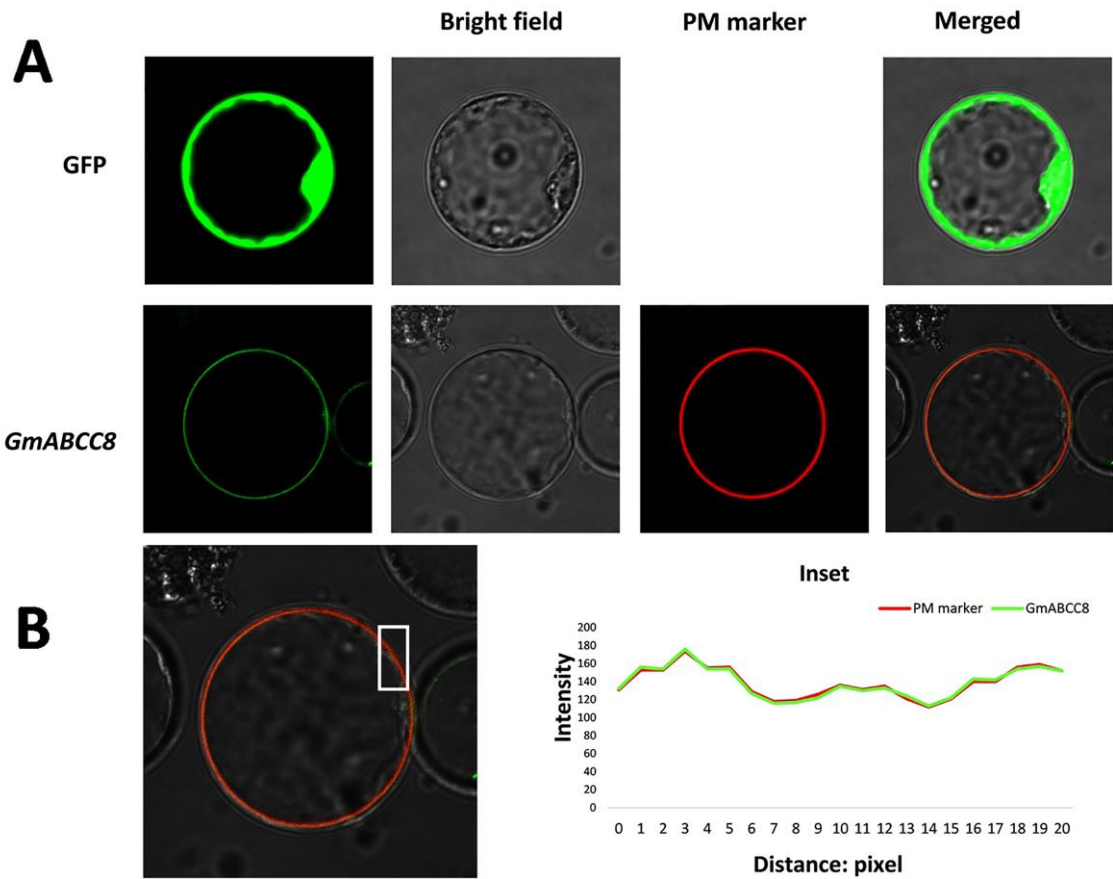
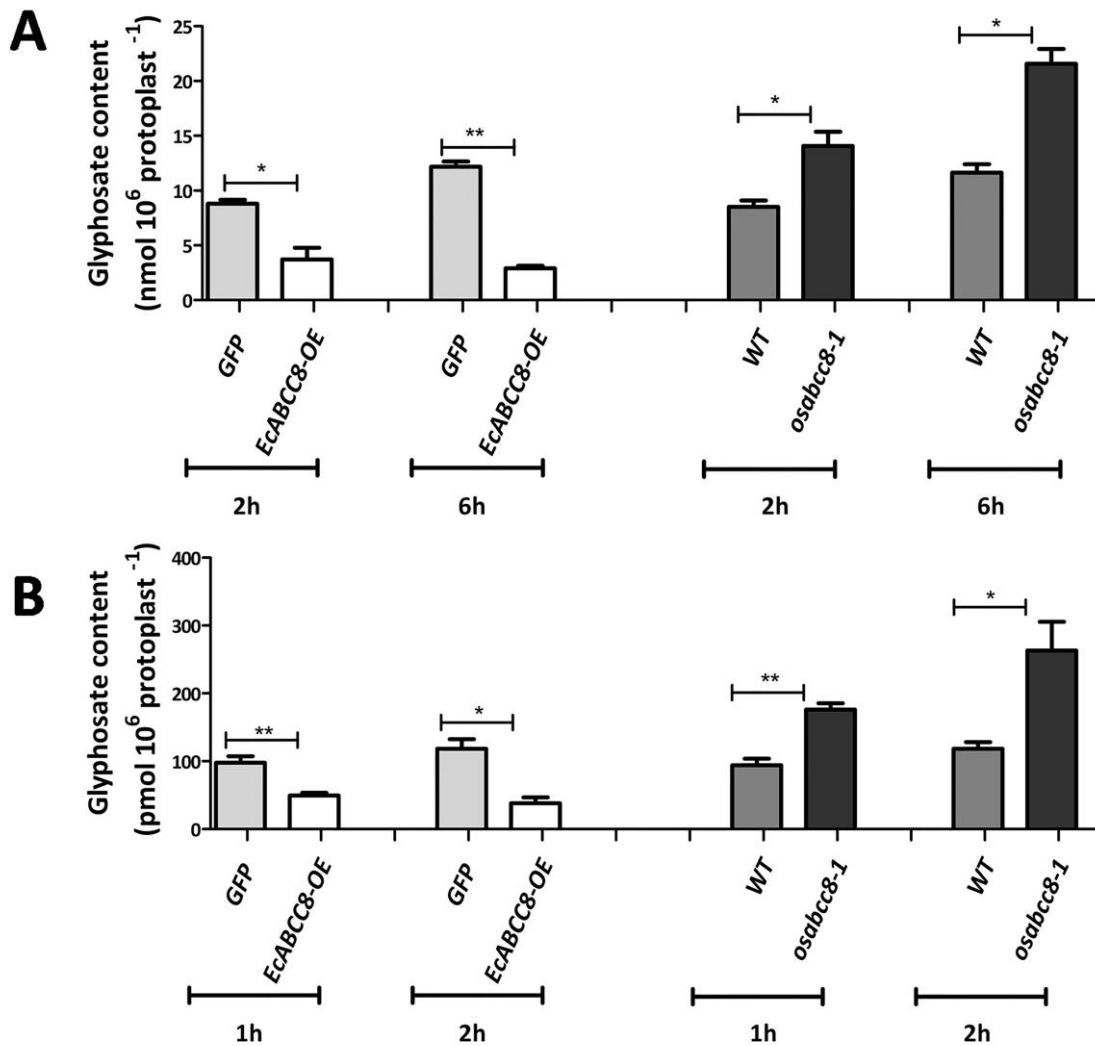**Figure S10.** Subcellular location of GmABCC8. (A) Co-localization of the GmABCC8 and the plasma membrane (PM) marker, and (B) Linescan analysis showing overlapping of fluorescence distribution of GmABCC8 (green) and the PM maker (red) in areas of interest (boxed).

Figure S11. Glyphosate content in rice leaf protoplasts of *EcABCC8*-OE vs *GFP*, and the ortholog knockout mutants of *osabcc8-1* vs wild type WT. (A) Intact plants were treated with glyphosate (68 g ha^{-1}) and then protoplasts isolated for glyphosate quantification, 2 and 6 h after treatment. (B) Protoplasts were isolated, then treated with glyphosate (60 μM), and glyphosate quantified 1 and 2h after treatment. Data are means ± SE (*n*=3). Significance of difference by the student t-test is indicated by *(*p*<0.05) and **(*p*<0.01). Two *EcABCC8*-OE and two knockout mutant lines were used in the experiments with similar results and hence only one set of data is presented.
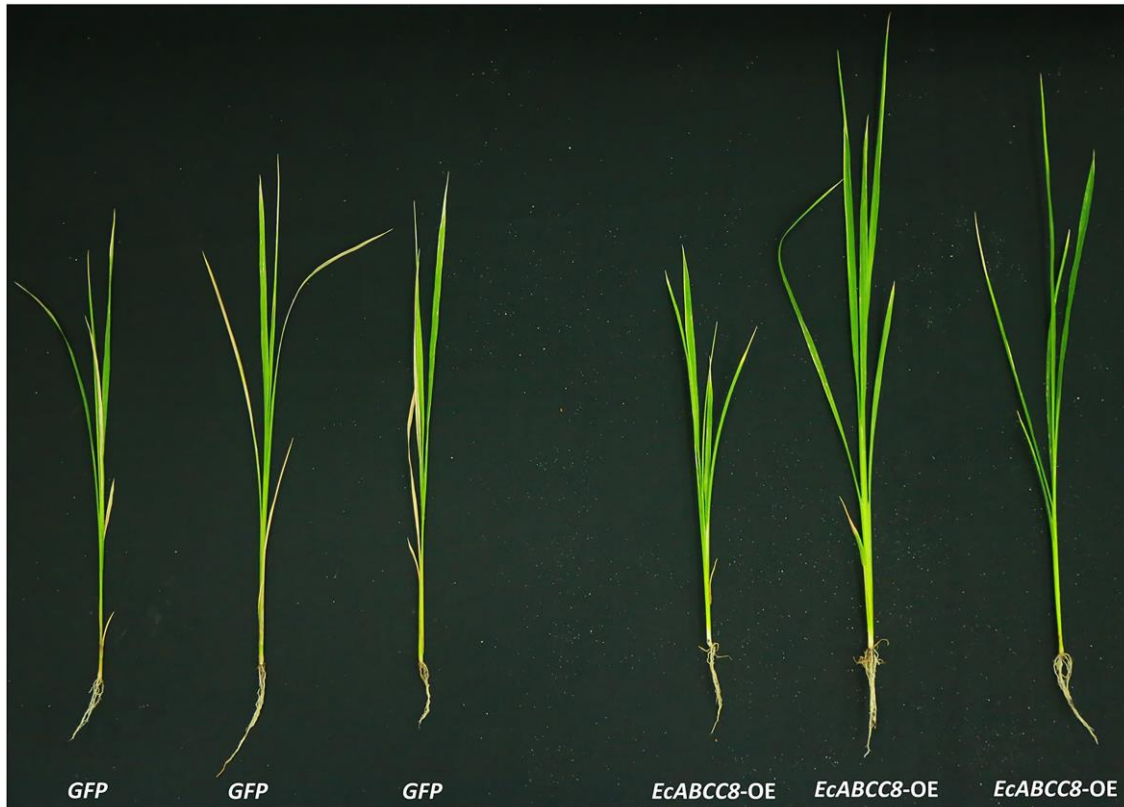
Figure S12. Leaf symptoms of rice plants expressing *EcABCC8* (*EcABCC8*–OE) versus *GFP* control, three weeks following glyphosate treatment (540 g ha^{-1}). Note the damage in leaf tips of *EcABCC8*-OE as compared to the damage across the whole leaves in *GFP* control.
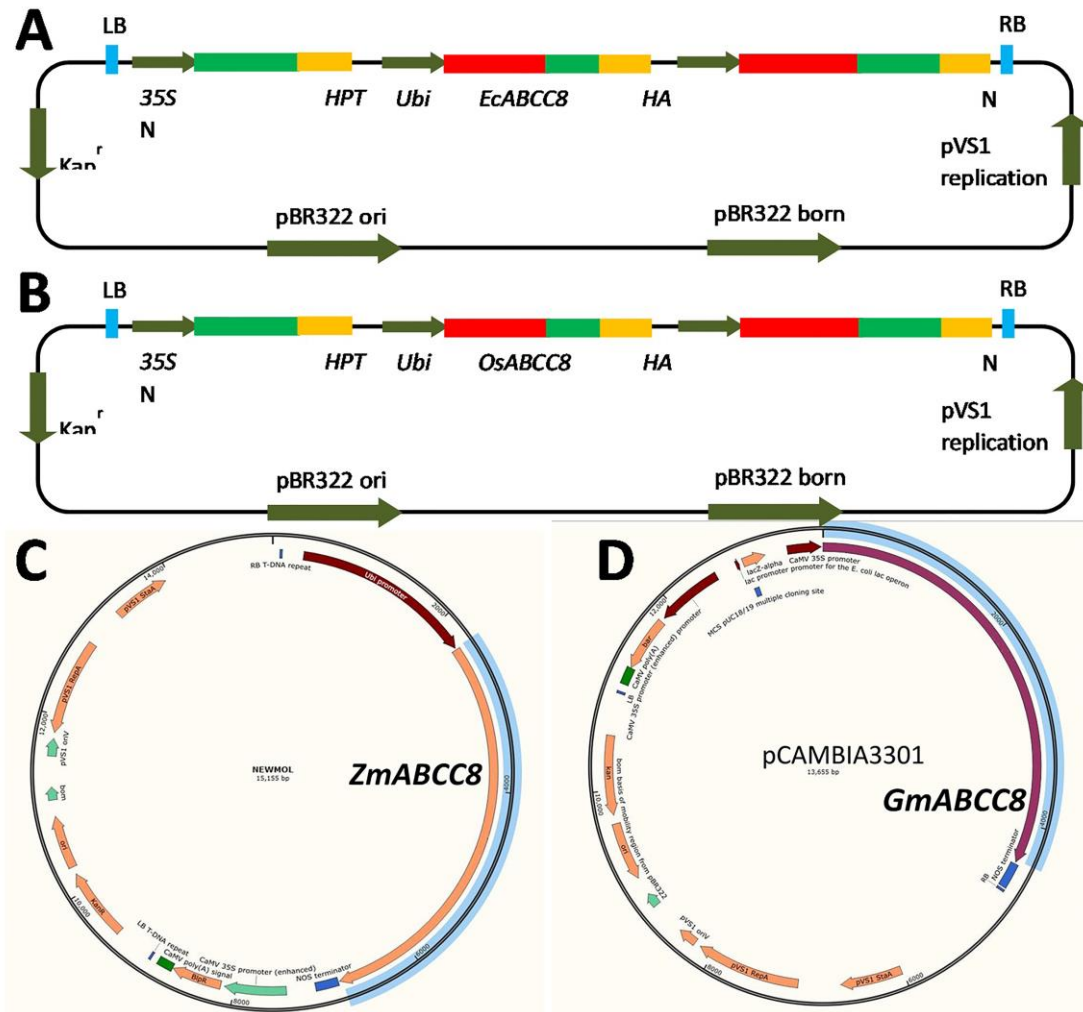
Figure S13. Vector construct for overexpression of the gene *EcABCC8* (A) and *OsABCC8* (B) in rice, *ZmABCC8* in maize (C), and *GmABCC8* in soybean (D).

1 **Table S1.** Primers used for RT-qPCR analysis of the membrane transporter genes in

2 *Echinochloa colona*

Gene_short_name	Direction	Sequence (5′–3′)
ABC transporter genes		
EC_v4.g002994	Forward	TCACCGTCCAGCATTAGTTG
	Reverse	GGCTTCAACACATCAAACTCTAC
EC_v4.g006991	Forward	GCACCGCTTGTTCTTAAAGG
	Reverse	GATTTCCCACTTCCTGTCCTC
EC_v4.g007634	Forward	TGACATGCTTACTGAACTCTCG
	Reverse	TCCAGACCCAGAATTTTGAGG
EC_v4.g009219	Forward	CTTGTCCTGGTCCTTAGTGATG
	Reverse	CATCCCACTCATATACACCTCG
EC_v4.g028874	Forward	AGCGATTCCTCTCCAAGTTC
	Reverse	ATAGGTGTTGAAGATGGTCGG
EC_v4.g029674	Forward	TGAAGTATCTTGGTGCCACTG
	Reverse	CTGGTGTGGTATCGGAGATTG
EC_v4.g039770	Forward	GATATGGCTGATTCCGAGAGTC
	Reverse	CGAGTGTTTCTTGGTATCTTTGC
EC_v4.g048404	Forward	ATTCTGGTAATGGAAGGCGG
	Reverse	ACTTGGTTCTGTTGACTGGC
EC_v4.g058209	Forward	TGATGCCGTCAGTTATCGTC
	Reverse	CTCCTTCTCAATCTCACCATACG
EC_v4.g069693	Forward	CCAACGAAGATGAAGGCAATG
	Reverse	GCTAGGGTGAGGTAATTCCAG
EC_v4.g071155	Forward	AGAGGCTCACTATTGCTGTTG
	Reverse	CCTTCCTGTGTCAACCATACTC
EC_v4.g084948	Forward	AGCGATTCCTCTCCAAGTTC
	Reverse	ATAGGTGTTGAAGATGGTCGG
EC_v4.g095434	Forward	GAGAGGTCATTCGTTCCAAGG
	Reverse	GCAATAAGTTGGCGTTGTCC
EC_v4.g098055	Forward	CGGCTGATTCTGAGGGTAATG
	Reverse	GGTAGGTCTTTCTCTTCAAGGG
EC_v4.g099458	Forward	ATGTTACGCTGGAAGATGGG
	Reverse	TGATGGAGAAGGCAAAGACG
EC_v4.g102032	Forward	AACGAGAGGAAAGAGAAATGGG
	Reverse	CGCAGCTAAGAAAATCATGTGG
Phosphate transporter genes		
EC_v4.g025847	Forward	GACGCCTACGACCTCTTCTG
	Reverse	CGAGGAAGGTGAGTATGAAGC
EC_v4.g065319	Forward	CAAAGCCGAAGGATCAATGC
	Reverse	GAAGACTCCAGCAATATACCCC

3

1 **Table S2.** Identification of differentially expressed membrane transporter genes in
2 glyphosate resistant (GR) and susceptible (S) *E. colona* using RNA sequencing
3 (RNA-seq)

Gene_short_name	RNA-seq		RT-qPCR validation	
	Fold change	Significance	Ratio (R/S)	Significance
ABC transporter genes				
EC_v4.g002994	1.8	*	1.7	*
EC_v4.g006991	**5.2**	******	**5.5**	******
EC_v4.g007634	1.7	*	1.8	*
EC_v4.g009219	1.6		1.5	*
EC_v4.g028874	1.6		1.7	*
EC_v4.g029674	1.6		1.5	*
EC_v4.g039770	**1.7**	*****	**6.0**	*****
EC_v4.g048404	**6.3**	******	**7.5**	******
EC_v4.g058209	2.4	*	3.1	*
EC_v4.g069693	2.4	*	2.5	*
EC_v4.g071155	1.8	*	2.1	
EC_v4.g084948	1.6		1.9	*
EC_v4.g095434	1.7	*	1.7	*
EC_v4.g098055	**9.0**	******	**10.3**	******
EC_v4.g099458	2.1	*	2.4	*
EC_v4.g102032	**7.4**	******	**11.5**	*****
Phosphate transporter genes				
EC_v4.g025847	2.9	*	2.5	
EC_v4.g065319	2.2	*	1.7	

4 *p*-value <0.05, 0.01 indicated by *, **.

5

6

1 **Table S3.** Quantitative RT-PCR validation of the candidate ABC transporter contigs

2 from *Echinochloa colona* using a series of pre-phenotyped samples. R: glyphosate

3 resistant, S: glyphosate susceptible

Sample sources	Relative expression Ratio (R/S)				
	EC_v4.g 098055	EC_v4.g 102032	EC_v4.g 006991	EC_v4.g 039770	EC_v4.g 048404
RNA-seq results (based on FPKM values)	9.0**	7.4**	5.2**	1.7*	6.3**
Validation of RNA-seq samples	10.3**	11.5*	5.5**	6.0*	7.5**
Validation of spare RNA-seq samples	12.5*	9.8*	4.8*	3.9*	8.1*
Population/line validation					
R_{bulk}/S_{bulk}	5.5**	4.0**	1.7*	1.6	1.7*
R_{single}/S_{single}	6.4*	7.1**	1.3	2.1	2.0*
R_{bulk}-R/R_{bulk}-S	2.5*	2.4*	1.0	0.7	1.0
R_{single}-R/R_{single}-S	2.7*	2.6*	1.4	2.4*	2.7
QBG1 (S) /S_{single}	0.2**	1.0	1.1	0.9	0.7
Crossy (S)/S_{single}	0.4	0.9	1.3	0.8	1.7
R_{single} (35/30C)/ R_{single} (25/20C)	2.8**	2.3*	1.2	0.7	1.3

4 *p*-value <0.05, 0.01 indicated by *, **.
5 FPKM: fragments per kilobase of exon per million fragments
6

7
8

9

10

11

Supplemental References

1. T.A. Gaines, A. Cripps, S.B. Powles, Evolved resistance to glyphosate in Junglerice (*Echinochloa colona*) from the tropical Ord Riverr-Region in Australia. *Weed Technol.* **26**, 480-484 (2012)..

2. S.S. Goh*, et al.*, Non-target-site glyphosate resistance in *Echinochloa colona* from Western Australia. *Crop Prot.* **112**, 257-263 (2018).

3. L. Pan*, et al.*, (2019) Aldo-keto reductase metabolizes glyphosate and confers glyphosate resistance in *Echinochloa colona*. *Plant Physiol.* **181**,1519-1534 (2019).

4. L. Guo*, et al.*, Echinochloa crus-galli genome analysis provides insight into its adaptation and invasiveness as a weed. *Nat. Commun.* **8**, 1031 (2017).

5. H. Han, Q. Yu, M.J. Owen, G.R. Cawthray, S.B. Powles, Widespread occurrence of both metabolic and target-site herbicide resistance mechanisms in *Lolium rigidum* populations. *Pest Manag. Sci.* **72**, 255-263 (2016).

6. T. Seiichi*, et al.*, (2010) Early infection of scutellum tissue with Agrobacterium allows high-speed transformation of rice. *Plant J.* **47**, 969-976 (2010).

7. Y.W. Zhang*, et al.*, Overexpression of a novel Cry1Ie gene confers resistance to Cry1Ac-resistant cotton bollworm in transgenic lines of maize. *Plant Cell Tiss. Org.* **115**, 151-158 (2013).

8. A. Kereszt*, et al.*, Agrobacterium rhizogenes-mediated transformation of soybean to study root biology. *Nature Protoc.* **2**, 948-952 (2007).

9. P.D. Hsu*, et al.*, DNA targeting specificity of RNA-guided Cas9 nucleases. *Nat. Biotechnol.* **31**, 827-832 (2013).

10. A. Nishimura, I. Aichi, M. Matsuoka, A protocol for Agrobacterium-mediated transformation in rice. *Nature Protoc.* **1**, 2796-2802 (2006).

11. X. Ma, L. Chen, Q. Zhu, Y. Chen, Y.G. Liu, Rapid Decoding of sequence-specific nuclease-induced heterozygous and biallelic mutations by direct sequencing of PCR Products. *Mol. Plant* **8**, 1285-1287 (2015).

12. R. Lister*, et al.*, Global epigenomic reconfiguration during mammalian brain development. *Science* **341**, 629-+ (2013).

13. D. Secco*, et al.*, Stress induced gene expression drives transient DNA methylation changes at adjacent repetitive elements. *eLife* **4**, 26 (2015).

14. Y. Xi, W. Li, BSMAP: whole genome bisulfite sequence MAPping program. *BMC bioinformatics* **10**, 232 (2009).

15. S.L. Zhong*, et al.*, Single-base resolution methylomes of tomato fruit development reveal epigenome modifications associated with ripening. *Nat. Biotechnol.* **31**, 154-159 (2013).

16. S.F. Geng*, et al.*, DNA methylation dynamics during the interaction of wheat progenitor Aegilops tauschii with the obligate biotrophic fungus Blumeria graminis f. sp. tritici. *New Phytol.* **221**, 1023-1035 (2019).

17. J. Ma*, et al.*, Disruption of OsSEC3A increases the content of salicylic acid and induces plant defense responses in rice. *J. Exp. Bot.* **69**, 1051-1064 (2018).

18. Y. Zhang*, et al.*, A highly efficient rice green tissue protoplast system for transient gene expression and studying light/chloroplast-related processes. *Plant Methods* **7**, 14 (2011).

19. C. Voelker, D. Schmidt, B. Mueller-Roeber, K. Czempinski, Members of the Arabidopsis AtTPK/KCO family form homomeric vacuolar channels in planta. *Plant J.* **48**, 296-306 (2006).

20. J.A. Gougler, D.R. Geiger, Uptake and distribution of N-phosphonomethylglycine in sugar beet plants. *Plant Physiol.* **68**, 668-672 (1981).

21. S.S. Goh, (2016) Quantitative estimation of fitness cost associated with glyphosate resistance in *Echinochloa colona*. PhD thesis, The University of Western Australia, (2016).

22. P.J. Larkin, Purification and viability determinations of plant protoplasts. *Planta* **128**, 213-216 (1976).

23. Q. Yu, S. Huang, S.B. Powles, Direct measurement of paraquat in leaf protoplasts indicates vacuolar paraquat sequestration as a resistance mechanism in *Lolium rigidum*. *Pestic. Biochem. Phys.* **98**, 104-109 (2010).

24. M.H. Denis, S. Delrot, Carrier-mediated uptake of glyphosate in broad bean (*Vicia faba*) via a phosphate transporter. *Physiol. Plantarum* **87**, 569-575 (1993).

25. N. Eswar*, et al.*, Comparative protein structure modeling using Modeller. *Curr. Protoc.*

Bioinformatics **5**, Unit-5.6 (2006).

26. A. Waterhouse*, et al.*, SWISS-MODEL: homology modelling of protein structures and complexes. *Nucleic Acids Res.* **46**, W296-W303 (2018).

27. A. Hildebrand, M. Remmert, A. Biegert, J. Söding, Fast and accurate automatic structure prediction with HHpred. *Proteins* **77**, 128-132 (2010).

28. L. Zimmermann*, et al.*, A completely reimplemented MPI bioinformatics toolkit with a new HHpred server at its core. *J. Mol. Biol.* **430**, 2237-2243 (2017).

29. Z.L. Johnson, J. Chen, Structural basis of substrate recognition by the multidrug resistance protein MRP1. *Cell* **168**, 1075-1085.e1079 (2017).

30. Z.L. Johnson, J. Chen, ATP binding enables substrate release from multidrug resistance protein 1. *Cell* **172**, 81-89.e10 (2018).

31. S. Potter*, et al.*, HMMER web server: 2018 update. *Nucleic Acids Res.* **46**, W200-W204 (2018).

32. L. Hoffer, D. Horvath, S4MPLE-sampler for multiple protein–ligand entities: simultaneous docking of several entities. *J. Chem. Inf. Model.* **53**, 88-102 (2013).

33. V. Zoete, M.A. Cuendet, A. Grosdidier, O. Michielin, SwissParam: A fast force field generation tool for small organic molecules. *J. Comput. Chem.* **32**, 2359-2368 (2011).

34. S. Jo, T. Kim, V.G. Iyer, W. Im, CHARMM-GUI: A web-based graphical user interface for CHARMM. *J. Comput. Chem.* **29**, 1859-1865 (2008).

35. M. Lomize, I. Pogozheva, H. Joo, H. Mosberg, A. Lomize, OPM database and PPM web server: Resources for positioning of proteins in membranes. *Nucleic Acids Res.* **40**, D370-376 (2011).

36. B. Das, H. Meirovitch, I.M. Navon, Performance of hybrid methods for large-scale unconstrained optimization as applied to models of proteins. *J. Comput. Chem.* **24**, 1222-1231 (2003).

37. M.J. Abraham*, et al.*, GROMACS: High performance molecular simulations through multi-level parallelism from laptops to supercomputers. *Softwarex* **1-2**, 19-25 (2015).

38. Z. Chu*, et al.*, Novel α-Tubulin mutations conferring resistance to dinitroaniline herbicides in *Lolium rigidum*. *Front. Plant Sci.* 9 (2018).

39. P.C. Do, E.H. Lee, L. Le, Steered molecular dynamics simulation in rational drug design. *J. Chem. Inf. Model.* **58**, 1473-1482 (2018).